Applied Catalysis B: Environmental 100 (2010) 179–183

Contents lists available at ScienceDirect

Applied Catalysis B: Environmental

journal homepage: www.elsevier.com/locate/apcatb

Significant photocatalytic enhancement in methylene blue degradation of TiO_2 photocatalysts via graphene-like carbon in situ hybridization

Yajun Wang, Rui Shi, Jie Lin, Yongfa Zhu*

Department of Chemistry, Tsinghua University, Beijing, 100084, China

ARTICLE INFO

Article history:
Received 16 May 2010
Received in revised form 19 July 2010
Accepted 24 July 2010
Available online 1 August 2010

Keywords:
Photocatalysis
Graphene-like carbon
TiO_2
Surface hybridization

ABSTRACT

Graphene-like carbon/TiO_2 photocatalysts were prepared via a facile in situ graphitization approach. The introduction of graphene-like carbon to TiO_2 effectively enhanced its photocatalytic activity. A graphene-like carbon/TiO_2 photocatalyst with a monolayer carbon shell (0.468 nm) showed the highest photocatalytic activity which is about 2.5 times as high as that of pristine TiO_2 (P25) under UV light irradiation. The mechanism of the enhanced photocatalytic activity is based on the synergetic effect between graphene-like carbon and TiO_2. The synergetic effect caused a rapid photoinduced charge separation and decreased the possibility of recombination of electron–hole pairs, which increased the number of holes participated in the photooxidation process and enhanced the photocatalytic activity.

1. Introduction

During the past decades, the photocatalysis has been extensively studied for water treatment because of its total destruction ability of pollutants and broad compound applicability [1]. Based on present researches, as a high-efficiency, nontoxicity, photochemical stability, low-cost photocatalyst, TiO_2 has been intensively investigated for complete degradation of recalcitrant organic pollutants [2–4]. However, the low quantum yield has hindered the application of this technology [5,6]. Therefore several methods have been employed to enhance the efficiency of the photocatalytic process of TiO_2, such as doping [7,8], codeposition of noble metals [9,10], and mixing of two semiconductors [11,12]. Though the above methods could partly enhance the photocatalytic activity of TiO_2, some key problems were still unsolved. For example, doped materials suffer from a thermal instability and an increase of carrier-recombination probability [7].

The delocalized conjugated π structures have been proven to cause a rapid photoinduced charge separation and a relatively slow charge recombination in electron-transfer processes [13]. Our group has developed conjugative π structure material hybridized semiconductor as efficient photocatalysts, such as C_{60} [14,15], polyaniline [16,17]. Graphene is a two-dimensional material, composed of single-, bi- and few- ($\leq$10) layers of carbon atoms forming six-membered rings [18]. It has attracted a great deal of scientific interest due to its outstanding mechanical, electrical, thermal, and optical properties [19]. Some studies have focused on applications of graphene-based materials in capacitors [20], biosensor [21], solar cells [22], liquid crystalline displays [23]. Graphene has a conjugated structure and the combination of TiO_2 and graphene may be an ideal system to achieve an enhanced charge separation in electron-transfer processes. To the best of our knowledge, few studies have been done on this topic. Recently, P25-TiO_2 dispersed on graphene nanosheet (synthesized by reduction from graphite oxide) was reported to show enhanced photocatalytic activity [24,25], however, the mechanism between graphene and semiconductor still need further study. Our group found that the conjugative π structure material coated on TiO_2 surface can obviously enhance the photocatalytic activity of TiO_2. On the present work, we developed a facile route to synthesize an in situ hybridized graphene-like carbon/TiO_2 (GT) photocatalyst. Melamine was used as the carbon source, which has a six-membered rings structure, and the N atoms can be removed to form graphene structure on the surface of TiO_2 in N_2 atmosphere prolonged heated. The in situ hybridization can achieve a tighter chemical binding between TiO_2 and graphene-like carbon. The chemical binding could provide a good spatial condition for charge transport from TiO_2 to graphene via the interfaces, and then achieved a higher photocatalytic activity. Besides, we have already carried out the research on TiO_2 modified by graphite-like carbon layers with a hydrothermal carbonization and an 800 °C graphitization process, using glucose as starting materials [26]. On this present work, the in situ hybridization method to form graphene-like carbon is more facile and could obtain a thinner carbon layer (graphene-like carbon). We found that

* Corresponding author. Tel.: +86 10 62787601; fax: +86 10 62787601.
E-mail address: zhuyf@tsinghua.edu.cn (Y. Zhu).

0926-3373/$ – see front matter © 2010 Published by Elsevier B.V.
doi:10.1016/j.apcatb.2010.07.028

photocatalysts have an optimal photocatalytic activity when they modified with a monomolecular layer of conjugative π structure material in our previous work [16,17]. Due to the unique and excellent electronic properties of graphene, the GT photocatalyst could achieve a higher photocatalytic activity. The as-prepared GT photocatalyst with monomolecular carbon layer (~0.468 nm) exhibited the highest photocatalytic activity which is 2.5 times as high as that of pristine TiO_2 (P25) under UV light irradiation. The structure between TiO_2 and graphene-like carbon as well as mechanism of enhanced photocatalytic activity were systematically investigated.

2. Experimental

2.1. Preparation of the GT photocatalyst

Melamine ($C_3H_6N_6$) was purchased from Sinopharm Chemical Reagent Corp, P.R. China; TiO_2 used to prepare GT photocatalysts was obtained from Degussa (P25 TiO_2, particle diameter 25 nm, surface area 50 m^2/g). All other reagents used in this research were analytical pure and used without further purification. The typical preparation of GT photocatalysts was as follows: Firstly, an appropriate amount of melamine was added into methanol then the beaker was placed in an ultrasonic bath for 30 min to make melamine totally disperse. The TiO_2 powder was added into the above solution and stirred in fume hood for 24 h. After volatilization of the methanol, opaque powder was obtained. Secondly, graphitization was achieved in a tube furnace by the powder calcined at 550 °C for 3 h in N_2 flow (60 mL/min). According to this method, different mass ratios of GT photocatalysts from 1 to 10% were synthesized. Pristine graphene-like carbon (graphene with some defects) was also prepared for comparison. Graphene-like carbon was prepared from reduction of graphene oxide according to literature [27,28].

To investigate the transition of photogenerated electrons before and after graphene-like carbon modification, TiO_2 and GT electrodes were prepared as follows: 5 mg of as-prepared photocatalyst was suspended in 5 mL ethanol to produce slurry, which was then dip-coated onto a 2 cm × 4 cm indium-tin oxide (ITO) glass electrode. Electrodes were exposed to UV light for 12 h to eliminate ethanol and subsequently calcined at 200 °C for 30 min under N_2 flow (rate = 60 mL/min). A standard three-electrode cell with a working electrode (as-prepared photocatalyst), a platinum wire counter electrode, and a standard calomel electrode (SCE) as reference electrode were used in photoelectric studies. And 0.1 M Na_2SO_4 was used as electrolyte solution. All investigated electrodes were of similar thickness (0.8–1 μm). Potentials are given with reference to the SCE.

2.2. Characterization

Raman spectra were determined on a Microscopic Confocal Raman Spectrometer (Renishaw, RM2000) using 632.8 nm as the light source. The high-resolution transmission electron microscopy (HRTEM) images were obtained by Tecnai TF20 transmission electron microscope operated at an accelerating voltage of 200 kV. UV–vis diffuse reflectance spectroscopy (DRS) was carried out on a Hitachi U-3010 UV-vis spectrophotometer. $BaSO_4$ was the reference sample. Thermogravimetric analysis and differential thermal analysis (TG-DTA) was performed in air at a heating rate of 10 °C/min on a Dupont 1090 thermal analyzer. X-ray photoelectron spectroscopy (XPS) was measured on a PHI 5300 ECSA instrument. The beam voltage was 3.0 kV, and the energy of Ar ion beam was 1.0 keV. Total organic carbon (TOC) was measured with a Tekmar Dohrmann Apollo 9000 TOC analyzer. The photoelectric performances were measured on an electrochemical system (CHI-660B, China). The photoresponses of the photocatalysts as UV light on and off were measured at 0.0 V. Electrochemical impedance spectra (EIS) were recorded in the open circuit potential mode. A sinusoidal ac perturbation of 5 mV was applied to the electrode over the frequency range of 0.05–10^5 Hz. SO_4^{2-}, NH_4^+ and NO_3^- ions were analyzed with an ion chromatograph (Shimadzu LC-10AS).

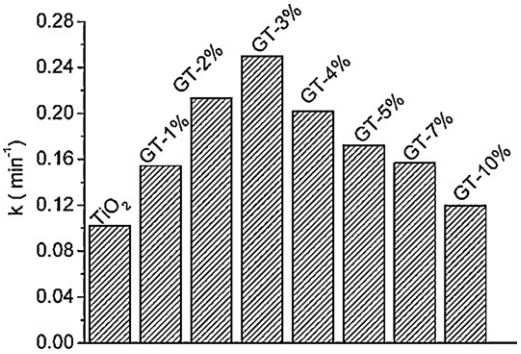

Fig. 1. The effect of graphene-like carbon content on MB degradation rate constants of TiO_2 and various GT photocatalysts (MB concentration = 10 mg/L).

2.3. Photocatalytic experiments

The photocatalytic activities were evaluated by the decomposition of methylene blue (MB) under UV light (λ = 254 nm). The radial flux was measured by a power meter from Institute of Electric Light Source, Beijing. UV light was provided by an 11 W UV-light lamp (Institute of Electric Light Sources, Beijing) and the average light intensity was 0.9 mW/cm^2. Aqueous suspensions of MB (100 mL, 10 mg/L) were placed in a vessel, and 50 mg GT photocatalyst was added. Prior to irradiation, the suspensions were magnetically stirred in dark for about 30 min. At certain time intervals, 2 mL aliquots were sampled and centrifuged to remove the particles. The filtrates were analyzed by recording variations of the maximum absorption peak (663 nm for MB) using a Hitachi U-3010 UV-vis spectrophotometer. The active species generated in the photocatalytic system could be detected through trapping by *tert*-butyl alcohol (*t*-BuOH) and ethylenediaminetetraacetic acid disodium salt (EDTA-Na).

3. Results and discussion

3.1. Enhancement of photocatalytic activity and photoelectrochemical properties

To analyze the synergetic effect of graphene-like carbon and TiO_2, the effect of graphene-like carbon content on photocatalytic degradation of GT photocatalysts was determined. It is well recognized that the photocatalytic degradation of organic pollutants follows pesudo-first-order kinetics [16]. We have derived the apparent reaction rate constants (k) for the degradation of MB from the linear slope of the relationship between $\ln(C/C_0)$ and t, where C_0 and C are the concentrations of initial solution and after t (min) of irradiation, respectively. The values of the degradation rate constants were shown in Fig. 1. The photocatalytic activity was enhanced gradually with increasing the proportion of graphene-like carbon. When the proportion of melamine got to 3.0%, the as-prepared photocatalyst had the optimal photocatalytic activity that could degrade MB by 73.7% in 5 min. The apparent rate constant k was 0.2483 min^{-1} and almost 2.5 times as high as that of pristine TiO_2 (P25). However, further increasing the proportion of melamine, the degradation rate decreased gradually though it remained higher than that of TiO_2 (P25). The modification had

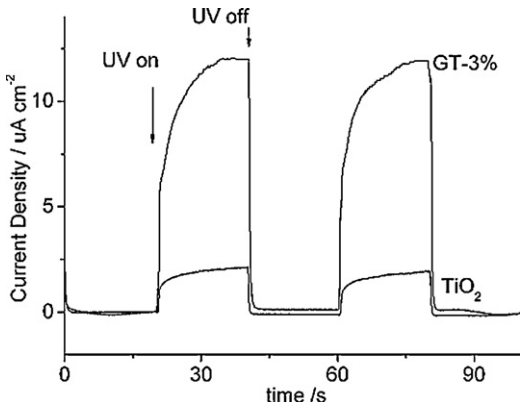

Fig. 2. The photoresponses of TiO_2 and GT-3% electrodes ([Na_2SO_4] = 0.1 M).

enhanced the photocatalytic activity of the TiO_2 implied that there may be some interaction between graphene-like carbon and TiO_2. The loading amount of graphene-like carbon had a great influence on the photocatalytic activity of the as-prepared photocatalysts. It can be inferred that at the mass ratio of 3.0%, the as-prepared photocatalyst had the optimal photocatalytic activity.

To further understand the mineralization property of the photocatalyst, the decrease of TOC in the photodegradation of MB by TiO_2 (P25) and GT-3% photocatalysts were determined. When 96% of MB was transformed in TiO_2 (P25) degradation in 30 min, about 51% of mineralized degree was reached. While 94% of MB was degraded by GT-3% in 15 min, about 65% of mineralized degree was achieved (see supplementary data Fig. S1). To more reliable to evaluate the photocatalytic activity, we investigated the formation of SO_4^{2-}, NO_3^- and NH_4^+ (see supplementary data Fig. S2). The concentrations of SO_4^{2-}, NO_3^- and NH_4^+ in GT system are all higher than that of TiO_2 system, confirming the photocatalytic activity of GT photocatalyst is higher than that of pristine TiO_2. After 30 min of irradiation, the concentration of SO_4^{2-} reached to 0.81 mg/L in GT system. Further increasing the irradiation time, the concentration of SO_4^{2-} did not exhibit significant increase. This result indicated that S atom was complete transformed in 30 min in graphene-like carbon/TiO_2 system. NO_3^- formation was insignificant, indicating NH_4^+ was the main product of nitrogen transformation for the photodegradation of MB.

Photoresponses were carried out for GT-3% and TiO_2 (P25) electrodes (Fig. 2). This photoresponsive phenomenon was entirely reversible. The photocurrent density of the GT-3% electrode was about five times as high as that of the TiO_2 (P25) electrode. This was consistent to the degradation experiment, and clearly indicated that the hybridization can improve the separation efficiency of photoinduced electrons and holes.

3.2. Structure and morphology of GT photocatalysts

Fig. 3 showed the HRTEM images of GT photocatalysts prepared with different mass ratios of melamine and TiO_2. It was found that the lattice structure of TiO_2 was very orderly and the outer boundary of the as-prepared sample was distinctly different from the TiO_2 core. The diameter of these as-prepared samples is about 25 nm (Fig. 3b) and it was not evidently different from the original TiO_2 (P25) (Fig. 3a). The measured distance between TiO_2 lattice planes is 0.351 nm which correspond to the interplanar spacing of anatase TiO_2 (101) plane. The thickness of graphene-like carbon layer coated on the GT-3% sample was about 0.468 nm (Fig. 3c), which is close to the scale of monolayer carbon (about 0.341 nm) [29]. Therefore, it can be speculated that the deposited graphene-like carbon layer on the surface of GT-3% was an approximately

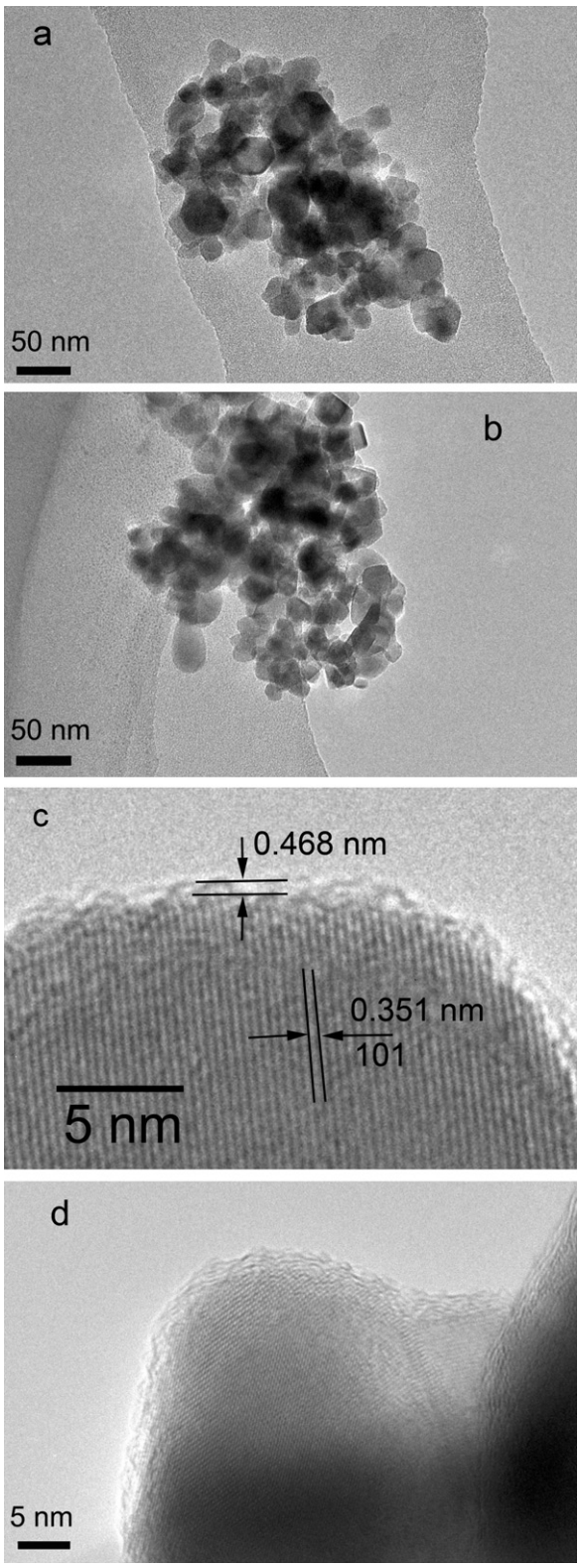

Fig. 3. The HRTEM images of TiO_2 and various GT photocatalysts: (a) TiO_2, (b and c) GT-3%, and (d) GT-10%.

monolayer structure. Since thickness of the graphene-like carbon layer of GT-10% is 2–3 nm (Fig. 3d), it was clearly that the GT-10% is a multilayer structure. Hence, it can be easily inferred from the HRTEM measurements that the thickness of the graphene-like carbon layer increased with increasing the melamine: TiO_2 mass ratio.

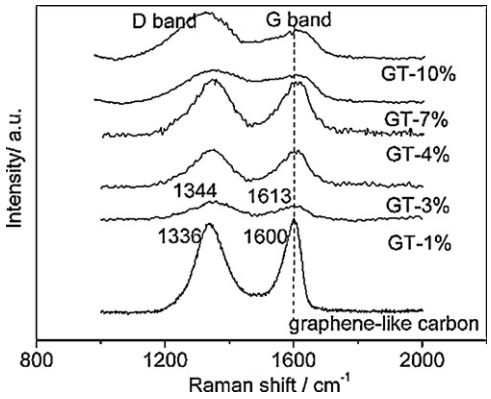

Fig. 4. Raman spectra of graphene-like carbon and various GT photocatalysts.

An estimate of the carbon content in the GT-3% sample could be obtained by TG-DTA, as shown in Fig. S3. The carbon content of GT-3% sample was calculated to be approximately 0.81 wt%, which was in agreement with the theoretical carbon content 0.86 wt% (carbon content in melamine was 28.57 wt%).

The UV–vis DRS spectra of GT photocatalysts comparing with that of TiO_2 (P25) was shown in Fig. S4. A sharp fundamental absorption edge rised at 400 nm as expected for TiO_2 (P25). The GT photocatalysts absorbed in the visible light region due to the presence of graphene-like carbon on the TiO_2 surface, while the absorption edge of TiO_2 can also be detected at 400 nm in the spectra of the GT photocatalysts. The absorption edge was not shifted for all GT samples, indicating identical band gap energies. In earlier reports, a decrease in band gap energy was observed for carbon doped TiO_2 due to the substitutional nature of the incorporated carbon [30]. In our work, most of the carbon in the GT samples was free, graphitic carbon. Hence an intense, broad background absorption in the visible light region instead of a band gap energy decrease was observed. With the increase of the carbon content in the GT samples, the absorption intensity became more pronounced.

The XPS spectra of GT photocatalysts were shown in Fig. S5. A single strong peak at 284.6 eV was attributed to carbon atoms (C–C bond) in a pure carbon environment. Melamine was used as the carbon source in this research; the N atoms can be removed to form graphene-like carbon structure on the surface of TiO_2 in N_2 atmosphere prolonged heated. Therefore, the peak ascribed to N 1s at around 398.2 eV and the peak related to C–N bond at around 288.3 eV were not detected. The peak ascribed to Ti–C bonds at around 281 eV was not detected in the GT photocatalysts, suggesting that carbon was not doped into the lattice of TiO_2. This result was in agreement with the UV–vis DRS spectra.

Fig. 4 shows the Raman spectra of the graphene-like carbon and GT photocatalysts. In the Raman spectra, it can be clearly seen that all samples exhibited characteristic peaks of graphene at around 1344 and 1613 cm^{-1}. The G-bands at around 1613 cm^{-1} could be attributed to the characteristic ordered graphitic carbon, and we were able to record well-defined G-bands for all our samples which confirmed the presence of sp^2-bonded carbon atoms in a two-dimensional hexagonal graphene layer. The D-band at around 1344 cm^{-1} could be assigned to the disordered graphitic carbon. Compared with the pristine graphene-like carbon (1600 cm^{-1}), the peak of G-band shifted to higher wavenumbers in all GT spectra. The shift in the Raman peak indicated that an intensive chemical interaction between graphene-like carbon and TiO_2 occurred.

The intensity of the G-band, associated with ordered graphitic carbon, is almost equivalent to that of the D-band. It suggested that graphitization reaction at 550 °C is not high enough to form a high ordered graphene structure. The intensity ratio of D- and G-band ($I_{D\text{-band}}/I_{G\text{-band}}$) was indicative of the degree of graphitization. The value for each sample was shown in Table 1, which further reflected the relative disorder and low graphitic crystallinity of the samples. The ratio increased with increasing carbon content, which indicated that samples with thinner carbon shells formed a more ordered carbon structure during the graphitization process.

Table 1
Degree of graphitization of GT photocatalysts.

Sample	Degree of graphitization $I_{D\text{-band}}/I_{G\text{-band}}$
GT-1%	1.06
GT-3%	1.02
GT-4%	1.08
GT-7%	1.27
GT-10%	1.66

3.3. Stability of the GT photocatalyst

To estimate the photostability of the GT photocatalyst, the recycled experiments for the photodegradation of MB were performed, and the results were shown in Fig. S6. After 20 h of photocatalytic degradation of MB, the GT-3% photocatalyst did not exhibit any significant loss of activity, confirming the GT photocatalyst is photostable during the photocatalytic degradation of the pollutant molecules. The HRTEM image of the GT-3% photocatalyst after 20 h photocatalytic reaction was also determined (Fig. S7). Compared with the HRTEM image before reaction (Fig. 3c), the image showed that the graphene-like carbon layer was not evident changed after 20 h photocatalytic reaction. These results all confirmed the stability of the as-prepared GT photocatalyst.

3.4. Mechanism on enhancement of photocatalytic activity

Fig. 5 showed the EIS Nynquist plots of TiO_2 (P25) and GT photocatalyst without and with UV irradiation. The arc radius on EIS Nynquist plot of the GT-3% is smaller than that of the TiO_2 (P25) with or without UV irradiation. Since the radius of the arc on the EIS spectra reflects the reaction rate occurring at the surface of electrode [31,32], it suggested that a more effective separation of photogenerated electron–hole pairs and a faster interfacial charge transfer occurred on GT photocatalyst under this condition [33]. This result clearly indicated that the combination of TiO_2 and graphene-like carbon could effectively enhance the separation of photogenerated electron–hole pairs.

The main oxidative species in photocatalytic process could be detected through the trapping experiments of radicals and holes. As shown in Fig. 6a, the addition of a scavenger of hydroxyl radicals (*t*-BuOH) [34] only caused small change in the photodegradation of MB. On the contrary, the photocatalytic activity of GT-3% could be

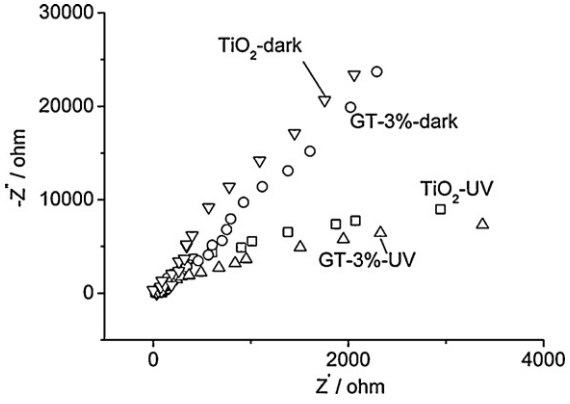

Fig. 5. EIS Nynquist plots of the TiO_2 and GT-3% photocatalysts.

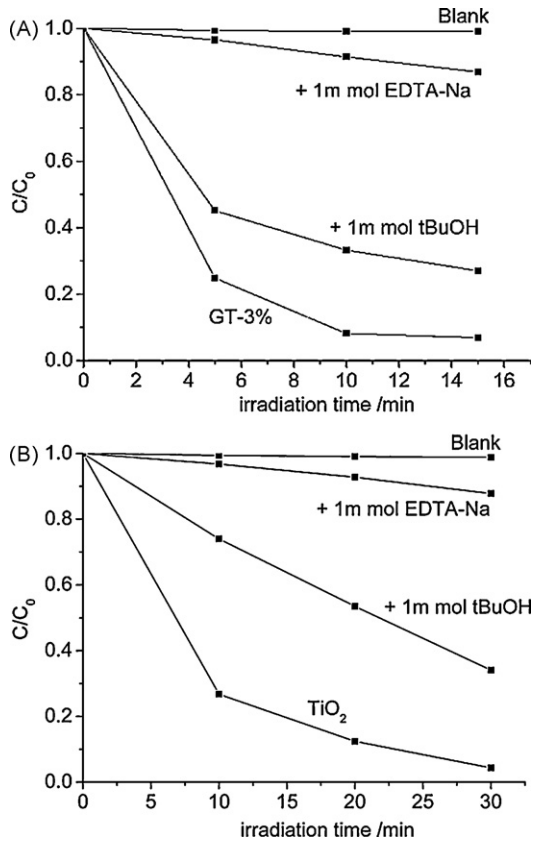

Fig. 6. The plots of photogenerated carriers trapping in the system of photodegradation of MB by (a) GT-3% and (b) TiO_2 under UV light irradiation.

greatly prevented by the addition of scavenger for holes (EDTA-Na) [34]. It clearly indicated that holes were the main active species of the GT photocatalyst, which could oxidize the adsorbed organic pollutants. The oxidative species of GT-3% photocatalyst is the same with TiO_2 (see Fig. 6b). It suggested that the oxidative species was not changed by introduction of graphene-like carbon to TiO_2.

As discussed above, the introduction of graphene-like carbon to the TiO_2 photocatalyst obviously enhanced photocatalytic activity. The Raman results indicated that a strong interaction existed between graphene-like carbon and TiO_2. Graphene is a good electron acceptor and transporter due to its two-dimensional conjugated π structure, the excited electrons of TiO_2 could transfer to graphene-like carbon. Thus, an effective charge separation was achieved and the possibility of the recombination of electron–hole pairs decreased. Besides, the oxidative species was not changed by introduction of graphene-like carbon to TiO_2. Therefore, the enhancement of photocatalytic activity could be attributed to the rapid photoinduced charge separation and the inhibition of recombination for electron–hole pairs, resulting in the increase of number of holes participated in the photooxidation process and enhancing of photocatalytic activity.

4. Conclusion

GT photocatalysts were prepared via an in situ graphitization approach. A GT photocatalyst with a carbon shell of monolayer (0.468 nm) showed the highest photocatalytic activity which is about 2.5 times as high as that of pristine TiO_2 (P25) under UV light irradiation. The synergetic effect between graphene-like carbon and TiO_2 caused a rapid photoinduced charge separation, which significantly enhanced the activity of the as-prepared GT photocatalysts. The sharply enhanced photocatalytic activity suggested the in situ graphitization could be one of the effective methods to improve the efficiency of the photocatalytic process.

Acknowledgements

This work was partly supported by Chinese National Science Foundation (20925725 and 20673065) and National Basic Research Program of China (2007CB613303).

Appendix A. Supplementary data

Supplementary data associated with this article can be found, in the online version, at doi:10.1016/j.apcatb.2010.07.028.

References

[1] A. Mills, S. Le Hunte, J. Photochem. Photobiol. A 108 (1997) 1–35.
[2] A. Fujishima, T.N. Rao, D.A. Tryk, J. Photochem. Photobiol. C 1 (2000) 1–21.
[3] K.I. Hadjiivanov, D.G. Klissurski, Chem. Soc. Rev. 25 (1996) 61–69.
[4] A. Heller, Acc. Chem. Res. 28 (1995) 503–508.
[5] H. Kominami, S.-Y. Murakami, J.-I. Kato, Y. Kera, B. Ohtani, J. Photochem. Photobiol. B 106 (2002) 10501–10507.
[6] J.C. Yu, L.Z. Zhang, Z. Zheng, J.C. Zhao, Chem. Mater. 15 (2003) 2280–2286.
[7] R. Asahi, T. Morikawa, T. Ohwaki, K. Aoki, Y. Taga, Science 293 (2001) 269–271.
[8] P.V. Kamat, Pure Appl. Chem. 74 (2002) 1693–1706.
[9] B. Kraeutler, A.J. Bard, J. Am. Chem. Soc. 100 (1978) 4317–4318.
[10] V. Subramanian, E.E. Wolf, P.V. Kamat, J. Am. Chem. Soc. 126 (2004) 4943–4950.
[11] H.G. Kim, P.H. Borse, W. Choi, J.S. Lee, Angew. Chem. Int. Ed. 44 (2005) 4585–4589.
[12] X. Fu, L.A. Clark, Q. Yang, M.A. Anderson, Environ. Sci. Technol. 30 (1996) 647–653.
[13] G. Yu, J. Gao, J.C. Hummelen, F. Wudl, A.J. Heeger, Science 270 (1995) 1789–1791.
[14] H. Fu, T. Xu, S. Zhu, Y. Zhu, Environ. Sci. Technol. 42 (2008) 8064–8069.
[15] S. Zhu, T. Xu, H. Fu, J. Zhao, Y. Zhu, Environ. Sci. Technol. 41 (2007) 6234–6239.
[16] H. Zhang, R. Zong, Y. Zhu, J. Phys. Chem. C 113 (2009) 4605–4611.
[17] H. Zhang, R. Zong, J. Zhao, Y. Zhu, Environ. Sci. Technol. 42 (2008) 3803–3807.
[18] C.N.R. Rao, K. Biswas, K.S. Subrahmanyam, A. Govindaraj, J. Mater. Chem. 19 (2009) 2457–2469.
[19] T.N. Lambert, C.A. Chavez, B. Hernandez-Sanchez, P. Lu, N.S. Bell, A. Ambrosini, T. Friedman, T.J. Boyle, D.R. Wheeler, D.L. Huber, J. Phys. Chem. C 113 (2009) 19812–19823.
[20] M.D. Stoller, S. Park, Y. Zhu, J. An, R.S. Ruoff, Nano Lett. 8 (2008) 3498–3502.
[21] X. Chen, C. Fu, W. Yang, Analyst 134 (2009) 2135–2140.
[22] N.L. Yang, J. Zhai, D. Wang, Y.S. Chen, L. Jiang, ACS Nano 4 (2010) 887–894.
[23] P. Blake, P.D. Brimicombe, R.R. Nair, T.J. Booth, D. Jiang, F. Schedin, L.A. Ponomarenko, S.V. Morozov, H.F. Gleeson, E.W. Hill, A.K. Geim, K.S. Novoselov, Nano Lett. 8 (2008) 1704–1708.
[24] H. Zhang, X. Lv, Y. Li, Y. Wang, J. Li, ACS Nano 4 (2009) 380–386.
[25] X.Y. Zhang, H.P. Li, X.L. Cui, Y. Lin, J. Mater. Chem. 20 (2010) 2801–2806.
[26] L.W. Zhang, H.B. Fu, Y.F. Zhu, Adv. Funct. Mater. 18 (2008) 2180–2189.
[27] Y.X. Xu, H. Bai, G.W. Lu, C. Li, G.Q. Shi, J. Am. Chem. Soc. 130 (2008) 5856–5857.
[28] D. Li, M.B. Muller, S. Gilje, R.B. Kaner, G.G. Wallace, Nat. Nanotechnol. 3 (2008) 101–105.
[29] S. Shanmugam, A. Gabashvili, D.S. Jacob, J.C. Yu, A. Gedanken, Chem. Mater. 18 (2006) 2275–2282.
[30] X.X. Wang, S. Meng, X.L. Zhang, H.T. Wang, W. Zhong, Q.G. Du, Chem. Phys. Lett. 444 (2007) 292–296.
[31] W.H. Leng, Z. Zhang, J.Q. Zhang, C.N. Cao, J. Phys. Chem. B 109 (2005) 15008–15023.
[32] H. Liu, S. Cheng, M. Wu, H. Wu, J. Zhang, W. Li, C. Cao, J. Phys. Chem. A 104 (2000) 7016–7020.
[33] X. Zhao, T. Xu, W. Yao, C. Zhang, Y. Zhu, Appl. Catal. B: Environ. 72 (2007) 92–97.
[34] C. Minero, G. Mariella, V. Maurino, D. Vione, E. Pelizzetti, Langmuir 16 (2000) 8964–8972.